



The Lumen of Human Intestinal Organoids Poses Greater Stress to Bacteria Compared to the Germ-Free Mouse Intestine: *Escherichia coli* Deficient in RpoS as a Colonization Probe

 Madeline R. Barron,^a  Roberto J. Cieza,^b David R. Hill,^c Sha Huang,^c Veda K. Yadagiri,^b  Jason R. Spence,^{c,d,e}
 Vincent B. Young^{a,b}

^aDepartment of Microbiology and Immunology, University of Michigan Medical School, Ann Arbor, Michigan, USA

^bDepartment of Internal Medicine, Division of Infectious Diseases, University of Michigan Medical School, Ann Arbor, Michigan, USA

^cDepartment of Internal Medicine, Division of Gastroenterology, University of Michigan Medical School, Ann Arbor, Michigan, USA

^dDepartment of Cell and Developmental Biology, University of Michigan Medical School, Ann Arbor, Michigan, USA

^eDepartment of Biomedical Engineering, University of Michigan Medical School, Ann Arbor, Michigan, USA

ABSTRACT Pluripotent stem-cell-derived human intestinal organoids (HIOs) are three-dimensional, multicellular structures that model a naive intestinal epithelium in an *in vitro* system. Several published reports have investigated the use of HIOs to study host-microbe interactions. We recently demonstrated that microinjection of the nonpathogenic *Escherichia coli* strain ECOR2 into HIOs induced morphological and functional maturation of the HIO epithelium, including increased secretion of mucins and cationic antimicrobial peptides. In the current work, we use ECOR2 as a biological probe to further characterize the environment present in the HIO lumen. We generated an isogenic mutant in the general stress response sigma factor RpoS and employed this mutant to compare challenges faced by a bacterium during colonization of the HIO lumen relative to the germ-free mouse intestine. We demonstrate that the loss of RpoS significantly decreases the ability of ECOR2 to colonize HIOs, although it does not prevent colonization of germ-free mice. These results indicate that the HIO lumen is a more restrictive environment to *E. coli* than the germ-free mouse intestine, thus increasing our understanding of the HIO model system as it pertains to studying the establishment of intestinal host-microbe symbioses.

IMPORTANCE Technological advancements have driven and will continue to drive the adoption of organotypic systems for investigating host-microbe interactions within the human intestinal ecosystem. Using *E. coli* deficient in the RpoS-mediated general stress response, we demonstrate that the type or severity of microbial stressors within the HIO lumen is more restrictive than those of the *in vivo* environment of the germ-free mouse gut. This study provides important insight into the nature of the HIO microenvironment from a microbiological standpoint.

KEYWORDS RpoS, colonization, intestine, organoid, stress


The mammalian gastrointestinal tract is inhabited by a diverse community of microbes that play critical roles in host development and health, including facilitating the development and maturation of the intestinal epithelial barrier (1–3). The intestinal epithelium represents an important physical and biochemical interface through which host-microbe symbioses within the gut are established and maintained (4). Historically, the model systems available to study intestinal epithelial-microbe interactions consisted primarily of immortalized cell lines and animal models. For instance, germ-free mice have become the gold standard for investigating host and microbial responses

Citation Barron MR, Cieza RJ, Hill DR, Huang S, Yadagiri VK, Spence JR, Young VB. 2020. The lumen of human intestinal organoids poses greater stress to bacteria compared to the germ-free mouse intestine: *Escherichia coli* deficient in RpoS as a colonization probe. *mSphere* 5:e00777-20. <https://doi.org/10.1128/mSphere.00777-20>.

Editor Marcela F. Pasetti, University of Maryland School of Medicine

Copyright © 2020 Barron et al. This is an open-access article distributed under the terms of the [Creative Commons Attribution 4.0 International license](https://creativecommons.org/licenses/by/4.0/).

Address correspondence to Vincent B. Young, youngvi@umich.edu.

 Maddie's first author paper is out! The lumen of human intestinal organoids poses greater stress to colonizing bacteria compared to the germ-free mouse intestine. @madelinerb2 @A2Binny

Received 30 July 2020

Accepted 23 October 2020

Published 11 November 2020

during the establishment of defined bacterial populations within the microbe-naive gut (5–10). However, technological advancements have expanded the repertoire of systems available for studying host-microbe interactions at the intestinal interface. In this regard, stem-cell-derived human intestinal organoids (HIOs) have emerged as powerful tools to investigate epithelial structure and function following initial interactions with a range of bacterial species (11–13).

HIOs are three-dimensional, organotypic structures comprised of multiple types of differentiated epithelial cells surrounded by a supporting mesenchyme (13–16). Derived from embryonic or induced pluripotent stem cells, HIOs possess many aspects of the microbe-naive intestinal epithelium in an experimentally tractable, *in vitro* system (13, 15, 16). We recently reported that microinjection of ECOR2, a nonpathogenic strain of *Escherichia coli* originally isolated from a healthy individual (17), into the lumen of HIOs induced transcriptional, morphological, and functional changes in HIOs resulting in the maturation of the epithelium (14). These changes included increased expression of genes regulating epithelial tight junction proteins, increased production of mucins, and secretion of antimicrobial peptides (14). Of note, *E. coli* established a stable population within the HIO lumen for several days after microinjection, with preservation of HIO epithelial barrier integrity (14). Overall, this study highlighted the utility of HIOs for studying epithelial adaptation to the establishment of bacterial populations at the intestinal epithelial interface. However, despite this demonstrated utility of HIOs, most studies have focused on epithelial responses, whereas less has been done to understand the HIO microenvironment from a microbiological standpoint. In the current work, we used *E. coli* as a biological probe to better characterize the HIO luminal environment from the perspective of a bacterial colonizer.

E. coli adapts to its environment via the well-characterized “general stress response,” which is regulated by the stress response sigma factor RpoS (18–20). Upon exposure to environmental stressors, including nutrient limitation, oxidative stress, and low pH (19), RpoS alters global bacterial gene expression to switch the cell from a state of active growth to one of survival (19). While RpoS has been extensively studied in the context of laboratory-imposed environmental stress, it has also been shown to facilitate bacterial colonization of the gut. For example, RpoS is important for efficient intestinal colonization by several pathogenic bacterial species, including *Vibrio cholerae*, *Salmonella enterica* serovar Typhimurium, and the virulent *E. coli* strain O157:H7 (21, 22). In addition, it was previously reported that RpoS may play a role in the initial establishment of nonpathogenic *E. coli* within the streptomycin-treated mouse gut (23). Given the role of RpoS in colonization of the intestine, we leveraged this information to compare the challenges faced by a bacterium when colonizing the HIO lumen and the murine gut. Using an isogenic $\Delta rpoS$ mutant of *E. coli* strain ECOR2, we demonstrate that the loss of RpoS attenuates the ability of ECOR2 to colonize HIOs, although it does not prevent colonization of germ-free mice. Rather, the $\Delta rpoS$ mutant exhibits a fitness defect in the mouse gut only in the context of microbial competition. Our results suggest that relative to the *in vivo* environment of the germ-free mouse intestine, the HIO lumen provides a greater challenge to *E. coli* during colonization. These results increase our understanding of the HIO model system as it pertains to studying intestinal epithelial-microbe interactions.

RESULTS

Generation and *in vitro* characterization of an isogenic $\Delta rpoS$ mutant of *E. coli* strain ECOR2. In this study, we used *E. coli* deficient in the RpoS-mediated stress response as a probe to better understand the HIO luminal environment from a microbiological standpoint. We generated an isogenic $\Delta rpoS$ mutant of *E. coli* strain ECOR2 (see Fig. S1A and B in the supplemental material) and first verified its phenotype by subjecting it to various *in vitro* stressors. RpoS is known to protect against exposure to low pH (19); thus, we tested the ability of the $\Delta rpoS$ mutant to survive incubation in LB broth adjusted to pH 2.5. As expected, the $\Delta rpoS$ mutant exhibited increased sensitivity to acid stress relative to the wild-type parent strain (Fig. 1A). Incubation for

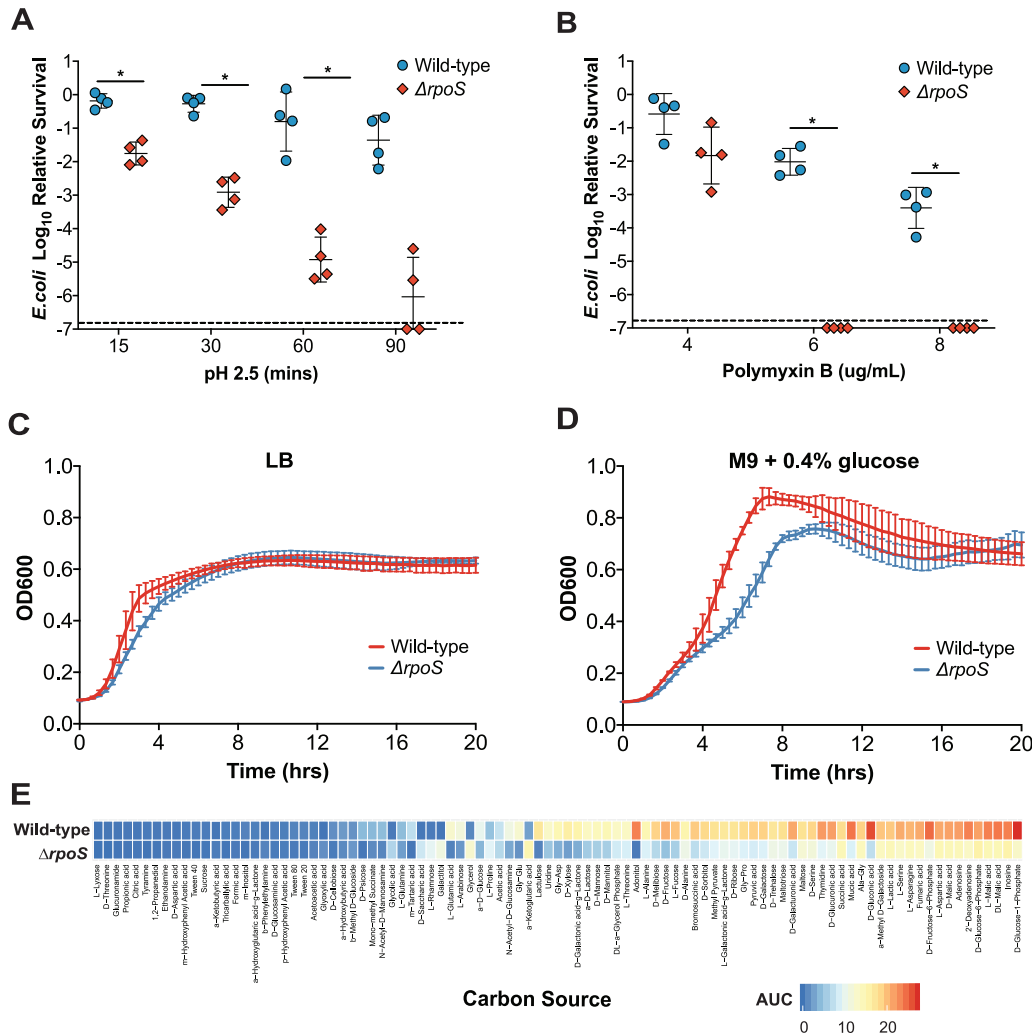


FIG 1 An isogenic $\Delta rpoS$ mutant of *E. coli* strain ECOR2 exhibits altered carbon metabolism and increased sensitivity to low pH, membrane stress, and nutrient limitation *in vitro*. (A and B) Wild-type ECOR2 and an isogenic $\Delta rpoS$ mutant were tested for survival after exposure to LB medium adjusted to pH 2.5 for 15, 30, 60, and 90 min and after 1 h of treatment with 4, 6, and 8 $\mu\text{g/ml}$ polymyxin B. Relative survival was calculated by dividing the CFU from the treated samples by those of the untreated control for each *E. coli* strain. The dashed line indicates the limit of detection ($n = 4$ biological replicates per *E. coli* strain for each assay). Values were log transformed prior to analysis. Error bars represent standard deviations of the means. *, $P < 0.05$ by a Mann-Whitney U test or Welch's unpaired t test depending on the data distribution. (C and D) Growth curves of wild-type ECOR2 and the $\Delta rpoS$ mutant in LB or M9 medium supplemented with 0.4% glucose were conducted at 37°C in a plate reader with shaking for 20 h. Error bars denote standard deviations of the means from at least 3 biological replicates per *E. coli* strain. (E) Growth of wild-type ECOR2 and the $\Delta rpoS$ mutant with 95 individual carbon sources using Biolog PM1 plates. The metabolic capacity of each strain, depicted as a heat map, is represented as the area under the curve (AUC) of OD_{595} values plotted over 24 h for each carbon source.

1 h in LB broth containing 4, 6, or 8 $\mu\text{g/ml}$ of polymyxin B, an antibiotic that binds lipopolysaccharide to destabilize bacterial membrane integrity (24), also revealed that the $\Delta rpoS$ mutant displayed a reduced ability to tolerate membrane stress compared to wild-type bacteria (Fig. 1B).

Previous studies have demonstrated that the loss of RpoS alters *E. coli* metabolism (25, 26). To this point, although the $\Delta rpoS$ mutant grew similarly to wild-type ECOR2 in LB broth (Fig. 1C), it exhibited a growth defect in minimal medium supplemented with glucose as a carbon source (Fig. 1D). Furthermore, a catabolic screen using Biolog PM1 (carbon nutrition) microplates revealed that the $\Delta rpoS$ mutant was defective in its ability to metabolize all 61 substrates that supported the growth of wild-type ECOR2 (Fig. 1E and Table S1). These data support that the loss of RpoS alters ECOR2 carbon metabolism and modulates growth depending on nutrient availability. Together, the

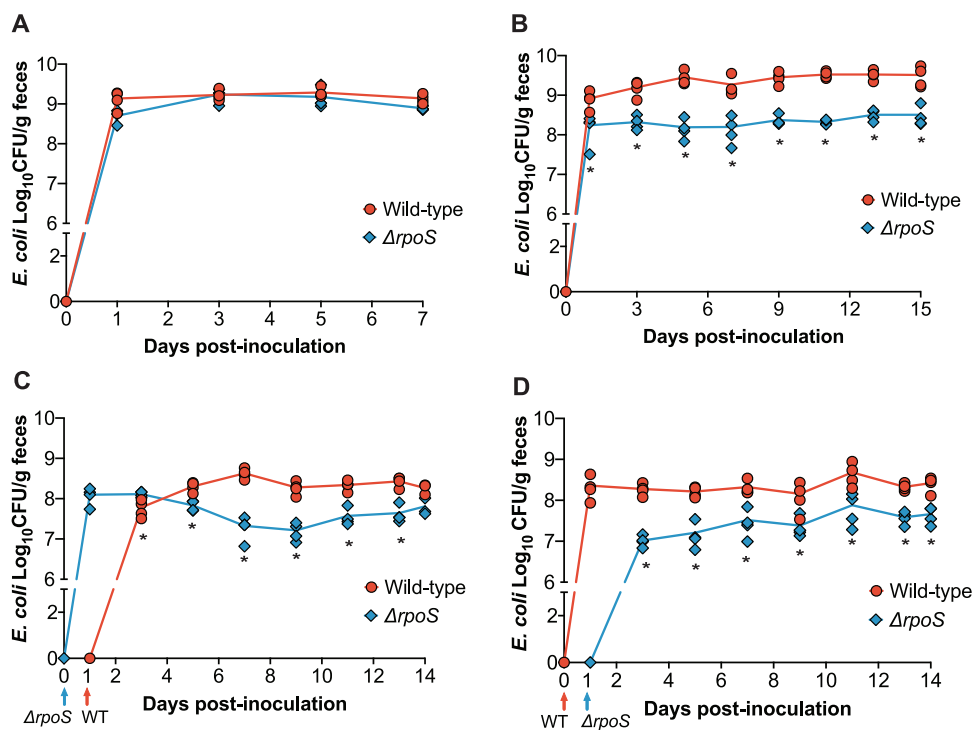


FIG 3 $\Delta rpoS$ ECOR2 exhibits a colonization defect in the germ-free mouse gut only in the context of microbial competition. Germ-free Swiss Webster mice were either monoassociated with 10^6 to 10^7 total CFU of wild-type or $\Delta rpoS$ mutant ECOR2 (A) or competitively inoculated with a 1:1 ratio of each strain together (B) or 24 h apart (C and D). At the indicated times, fecal samples were homogenized, diluted, and plated as described in Materials and Methods ($n = 3$ to 4 mice per time point). *, $P < 0.05$ by Mann-Whitney U tests. WT, wild type.

gut from the perspective of a bacterial colonizer. In *E. coli* and other Gram-negative bacteria, the ability to respond to diverse stressors in the environment, including within the gut, occurs via the RpoS-mediated stress response (18–23). Indeed, our data demonstrate that the loss of RpoS decreases the ability of *E. coli* strain ECOR2 to withstand membrane stress and exposure to low pH as well as alters its capacity to metabolize a broad range of carbon substrates. Importantly, we found that the loss of RpoS significantly decreased the ability of ECOR2 to colonize HIOs, though it did not prevent colonization of germ-free mice. These data indicate that the type or severity of microbial stressors within the HIO lumen is more restrictive than those of the *in vivo* intestinal environment.

There are likely a number of factors that shape the distinct environment of the HIO lumen. We have shown that the HIO epithelium produces antimicrobial peptides, which could be particularly stressful to microbes within the small, static luminal space (14). To this point, since there is no peristalsis and luminal flow within HIOs, this leads to a buildup of epithelial and microbe-derived waste within the HIO lumen (28). In this regard, technological advancements that establish steady-state liquid flow through the HIO lumen (28) may lessen or eliminate microbial stressors within the HIO microenvironment. Given our Biolog data demonstrating that the $\Delta rpoS$ mutant has a limited nutritional repertoire relative to wild-type ECOR2, another hypothesis is that the HIO lumen is more restricted in terms of nutrient availability than the murine intestine. Indeed, the mouse gastrointestinal tract contains a relatively rich nutrient pool that is replenished during regular feeding (29, 30). Furthermore, several studies have demonstrated that nutrient availability is the primary driver of *E. coli* colonization and adaptation within the murine gut (9, 31, 32). Thus, nutrient availability may explain the colonization dynamics observed *in vivo*, where the $\Delta rpoS$ mutant grew to wild-type levels during monoassociation of germ-free mice yet displayed a colonization defect in the context of microbial competition. The nutrient milieu of HIOs is relatively unknown,

TABLE 1 Bacterial strains, plasmids, and primers used in this study

<i>E. coli</i> strain, primer, or plasmid	Relevant characteristic(s) and/or sequence (5'–3')	Reference
<i>E. coli</i> strains		
ECOR2	Nonpathogenic <i>E. coli</i> strain isolated from a healthy individual	17
ECOR2 $\Delta rpoS$	ECOR2 <i>rpoS</i> disrupted with a <i>neo</i> cassette; Km ^r	This study
Primers		
MB001-F	ATGAGTCAGAATACGCTGAAAGTTTCATGATTTAAATGAAGATCGGAATT; for lambda red replacement	This study
MB001-R	TTACTCGCGGAACAGCGCTTCGATATTCAGCCCTGCGTTTGACGAGATTT; for lambda red replacement	This study
MB002-F	ATGAGTCAGAATACGCTGAAAGTTC; forward primer to amplify <i>rpoS</i> ; product length, 993 bp	This study
MB002-R	TTACTCGCGGAACAGCGCTTCGATA; reverse primer to amplify <i>rpoS</i>	This study
MB003-F	CCAGTTCAACAGCTTGCAT; forward primer for Sanger sequencing (123 bp upstream of <i>rpoS</i>); product length, 1.25 kb	This study
MB003-R	GTGCGTATGGGCGTAATTT; reverse primer for Sanger sequencing (95 bp downstream of <i>rpoS</i>)	This study
<i>rpoS</i> -RT-F	CCTGGCCGATGAAAAGAG; forward primer for qRT-PCR analysis of <i>rpoS</i> expression; product length, 81 bp	37
<i>rpoS</i> -RT-R	AACAGCCATTTGACGATGCTC; reverse primer for qRT-PCR analysis of <i>rpoS</i> expression	37
<i>rpoA</i> -F	ATGCAGGGTCTGTGACAGA; forward primer to amplify <i>rpoA</i> for qRT-PCR; product length, 140 bp	38
<i>rpoA</i> -R	AGAATACGGCGCAGTGCATT; reverse primer to amplify <i>rpoA</i> for qRT-PCR	38
Plasmids		
pKD46	Temp-sensitive Red+Gam-expressing plasmid; Ap ^r	34
pKD4	Template plasmid containing the <i>neo</i> gene template; Km ^r Ap ^r	34

though it is presumably derived from the surrounding culture medium that has been further modified by the metabolic activities of the epithelium (33) and mesenchyme. Therefore, the diversity and concentration of substrates available for *E. coli* consumption within HIOs are potentially limited. Ultimately, we suspect that there are a number of conditions that together create the relatively hostile environment within HIOs. More extensive work is required to characterize the exact nature of the nutritional or epithelial-derived microbial stressors inherent to the HIO lumen.

Overall, we have demonstrated that, from a bacterial standpoint, HIOs possess a unique luminal environment relative to the germ-free mouse intestine. Our results indicate that the type or severity of microbe-perceived stress within the HIO lumen is more restrictive than that of the *in vivo* gut environment. As organotypic models continue to be employed for investigating intestinal host-microbe interactions, it is critical that we benchmark these systems so that experiments can be put into proper perspective. Moving forward, the results from this study will better inform when and how we use HIOs to investigate diverse aspects of host-microbe symbioses within the gut.

MATERIALS AND METHODS

Bacterial strains and plasmids. Strains and plasmids are listed in Table 1. *Escherichia coli* strain ECOR2 (ATCC 35321) (17) was used in the present study. An isogenic $\Delta rpoS$ mutant was constructed by disruption of the ECOR2 *rpoS* gene via lambda red-mediated gene replacement with the aminoglycoside phosphotransferase gene (*neo*), which encodes resistance to kanamycin (34). The *neo* gene was amplified from the plasmid pKD4 (34) using primers MB001-F and MB001-R. The *neo* PCR product containing 50 bases upstream and downstream homologous to those of the *rpoS* gene was subsequently electroporated into ECOR2 containing plasmid pKD46, which contains the phage lambda Red recombinase gene cluster (34). Successful disruption of the *rpoS* gene was verified by endpoint PCR using primers MB002-F and MB002-R. Sanger sequencing was conducted with primers MB003-F and MB003-R, and real-time reverse transcription-quantitative PCR (qRT-PCR) was performed with primers *rpoS*-RT-F and *rpoS*-RT-R (see below and Fig. S1A and B in the supplemental material). Bacteria were grown aerobically in LB broth or on LB agar at 37°C. In all experiments, medium was supplemented with kanamycin sulfate (50 μ g/ml) for growth of the $\Delta rpoS$ mutant.

qRT-PCR. qRT-PCR was used to verify the loss of *rpoS* expression in the $\Delta rpoS$ ECOR2 mutant. Cultures of wild-type and $\Delta rpoS$ ECOR2 grown overnight were diluted 1:100 in sterile LB broth. After 8 h of incubation, 1 ml of each culture was added to 2 ml RNeasy lysis reagent (Qiagen) according to the manufacturer's instructions. This time point was chosen because it correlates with entry into the stationary phase of growth (Fig. 1C and D), when RpoS is most abundant in the cell (19, 35). Samples were stored at –20°C until RNA extraction. RNA was extracted from each sample using the RNeasy minikit (Qiagen) and quantified with the Quant-IT RiboGreen RNA assay kit (Invitrogen). One microgram of RNA was reverse transcribed to cDNA with the QuantiTect reverse transcription kit (Qiagen) according to the manufacturer's instructions. For qRT-PCR analyses, 20- μ l reaction mixtures were prepared using the QuantiTect SYBR green PCR kit (Qiagen) and primers *rpoS*-RT-F and *rpoS*-RT-R. qRT-PCR was

performed on a LightCycler96 qPCR machine (Roche) with 45 cycles of 94°C for 15 s, 53°C for 30 s, and 72°C for 30 s. The relative expression level of *rpoS* was determined via the $\Delta\Delta C_T$ method using *rpoA* as the control gene (amplified with *rpoA-F* and *rpoA-R*). All reactions were followed by a melting curve to determine amplicon purity.

Phenotypic analyses. For growth curve analyses, cultures of wild-type ECOR2 and the isogenic $\Delta rpoS$ mutant grown overnight were diluted to an optical density at 600 nm (OD_{600}) of 0.01 in either sterile LB broth or M9 minimal medium containing 0.4% glucose. Two hundred microliters of each culture was transferred into a clear, flat-bottomed, 96-well microplate. At least six technical replicates were included per experiment. A VersaMax microplate reader (Molecular Devices, LLC, Sunnyvale, CA) was used to measure the OD_{600} at 20-min intervals in microplates maintained at 37°C with regular shaking over a 20-h time course.

To assess the ability of the $\Delta rpoS$ mutant to withstand stress *in vitro*, cultures of the $\Delta rpoS$ mutant and its wild-type parent strain grown overnight were diluted 1:100 in sterile LB broth and grown to mid-log phase (OD_{600} of ~0.5 to 0.6). For membrane stress experiments, 500 μ l of each culture was then treated with either 4, 6, or 8 μ g/ml polymyxin B or water (as a control) and incubated for 1 h. Polymyxin B binds lipopolysaccharide to destabilize the membrane of Gram-negative bacteria (24). For pH stress assays, bacterial cultures were centrifuged at $4,000 \times g$ for 5 min, and 1 ml of cells was then centrifuged a second time and resuspended in LB broth with a pH of 2.5 (adjusted with HCl). Cells were then incubated without shaking at 37°C for 15, 30, 60, and 90 min. Surviving cells were enumerated by serial plating on LB agar.

The metabolic properties of wild-type and $\Delta rpoS$ mutant ECOR2 were assessed with Biolog PM1 plates according to the manufacturer's instructions. Bacteria grown overnight on LB agar were resuspended in Biolog inoculating fluid to a final OD_{600} of 1.0. Each well of the Biolog plate was inoculated with 100 μ l of the cell suspension and incubated in a BioTek kinetic plate reader (BioTek Instruments, Winooski, VT) for 24 h. The OD_{595} was used to measure the reduction of tetrazolium violet dye every 15 min. The area under the curve (AUC) of the OD_{595} values was calculated as a measure of bacterial oxidation for each carbon source tested and plotted over time.

HIO generation and experimentation. HIOs (13, 16) were generated as described previously (14) and maintained in medium containing epidermal growth factor (EGF), Noggin, and R-spondin (ENR medium [see reference 15]) in Matrigel (8 mg/ml) without antibiotics prior to microinjection experiments. Bacterial cultures for microinjection were prepared by incubating wild-type ECOR2 and the $\Delta rpoS$ mutant overnight at 30°C with low shaking. The following day, cultures had reached an OD_{600} of ~1.0 and were diluted 1:10 in sterile phosphate-buffered saline (PBS) and centrifuged for 10 min at $4,000 \times g$. Bacterial cells were then resuspended in sterile PBS. One hundred ninety microliters of this suspension was mixed with 10 μ l of 4-kDa fluorescein isothiocyanate (FITC)-dextran suspended in PBS (2 mg/ml). FITC-dextran acted as a marker to ensure that HIOs were successfully microinjected and that the epithelial barrier remained intact (see below).

To introduce bacteria into the lumen of HIOs, microinjection was performed using thin-walled glass capillaries mounted on a Xeneworks micropipette holder with analog tubing, as previously described (11, 14). Each HIO was microinjected with approximately 10^4 CFU of wild-type ECOR2 or the isogenic $\Delta rpoS$ mutant. After microinjection, HIOs were incubated for 1 h at 37°C. To remove bacteria introduced into the culture medium during the microinjection process, HIO culture medium was removed, and cultures were rinsed with PBS and washed with ENR medium containing 15 μ g/ml gentamicin. HIOs were then washed again in PBS, and the medium was replaced with fresh antibiotic-free ENR medium. Successful microinjection was verified by visualizing the fluorescence of FITC-dextran in each HIO several hours after microinjection using an Olympus IX71 epifluorescence microscope. HIOs were considered successfully microinjected if an FITC signal was detectable. An absence of fluorescence was indicative of a loss of HIO structural integrity, and these organoids were excluded from further analyses.

Bacteria were enumerated in the HIO lumen as previously described (36). Briefly, HIO culture medium was removed from wells, and each organoid was placed into individual screw-cap tubes containing 300 μ l PBS and 1.0-mm Biospec zirconia/silica beads (Fisher Scientific). HIOs were homogenized for 30 s in a Mini Bead Beater 8 instrument (Biospec Products). Viable bacteria were enumerated via serial plating of the homogenate on LB agar.

Germ-free mouse colonization. All animal experiments were performed with approval from the University Committee on Use and Care of Animals at the University of Michigan. Groups within an experiment were age matched to the greatest extent possible. Male and female germ-free Swiss Webster mice aged 6 to 9 weeks were obtained from a colony established and maintained by the University of Michigan Germ-Free Mouse Facility. Mice received sterile food, water, and bedding and remained bacteriologically sterile (except for the experimental *E. coli* strains) throughout the course of the experiments. Bacterial inocula were prepared as follows. Wild-type ECOR2 and the $\Delta rpoS$ mutant were grown in LB broth overnight at 30°C with low shaking. By the next morning, cultures had reached an OD_{600} of approximately 1.0. Cultures were then diluted 1:10 in sterile PBS and centrifuged at $4,000 \times g$ for 10 min. The supernatant was discarded, and cells were resuspended in sterile PBS. Mice were inoculated via oral gavage with 100 μ l of the bacterial suspension, which equated to about 10^6 to 10^7 CFU per mouse of each strain for monocolonization experiments and 10^6 CFU per mouse of each strain administered together or sequentially (i.e., 24 h apart) for competition experiments, where indicated. To differentiate between wild-type and mutant growth, feces were collected and serially plated on LB agar with and without kanamycin sulfate (50 μ g/ml). Feces were collected every other day for 7 days (monoassociation studies) or 14 to 15 days (competition experiments).

Statistical analyses. AUC values for Biolog assays and the corresponding heat map were generated using custom R scripts (https://github.com/barronmr/Biolog_AUC.git). All other analyses were performed using GraphPad Prism 8.3 (GraphPad Software, Inc.). When comparing two groups, a Welch's unpaired *t* test was used for normally distributed data, and a Mann-Whitney U test was used for data that were not normally distributed. A *P* value of ≤ 0.05 was considered significant. Adobe Illustrator CC 2020 was used to arrange panels and generate the final figures.

SUPPLEMENTAL MATERIAL

Supplemental material is available online only.

FIG S1, EPS file, 2 MB.

TABLE S1, DOCX file, 0.02 MB.

ACKNOWLEDGMENTS

We acknowledge the University of Michigan Germ-Free Mouse Core for assistance with mouse colonization experiments. We also thank Stephanie Thiede and Emily Benedict for providing R scripts for Biolog assay analyses as well as the laboratories of Mary O'Riordan and Harry Mobley for sharing bacterial strains and equipment. Finally, we thank Kimberly Vendrov, Annie Pinchkoff, Michelle Sydney Smith, and Pariyamon Thaprawat for experimental assistance.

This work was funded by National Institutes of Health cooperative agreement AI116482 to V.B.Y. and J.R.S. and AI007528 to M.R.B. The funders had no role in study design or data collection and interpretation.

V.B.Y. has served as a consultant to Vedanta Biosciences, Bio-K+ International, and Panteryx.

M.R.B., R.J.C., and V.B.Y., conception or design of work; M.R.B., R.J.C., D.R.H., S.H., and V.K.Y., data collection; M.R.B. and R.J.C., data analysis; M.R.B. and V.B.Y., drafting the article; M.R.B., R.J.C., D.R.H., S.H., V.K.Y., J.R.S., and V.B.Y., critical revision of the manuscript; M.R.B., R.J.C., D.R.H., S.H., V.K.Y., J.R.S., and V.B.Y., final approval of the version to be published.

REFERENCES

- Flint HJ, Scott KP, Louis P, Duncan SH. 2012. The role of the gut microbiota in nutrition and health. *Nat Rev Gastroenterol Hepatol* 9:577–589. <https://doi.org/10.1038/nrgastro.2012.156>.
- Turroni F, Milani C, Duranti S, Lugli GA, Bernasconi S, Margolles A, Di Pierro F, van Sinderen D, Ventura M. 2020. The infant gut microbiome as a microbial organ influencing host well-being. *Ital J Pediatr* 46:16. <https://doi.org/10.1186/s13052-020-0781-0>.
- Young VB. 2017. The role of the microbiome in human health and disease: an introduction for clinicians. *BMJ* 356:j831. <https://doi.org/10.1136/bmj.j831>.
- Soderholm AT, Pedicord VA. 2019. Intestinal epithelial cells: at the interface of the microbiota and mucosal immunity. *Immunology* 158:267–280. <https://doi.org/10.1111/imm.13117>.
- Bhattarai Y, Kashyap PC. 2016. Germ-free mice model for studying host-microbial interactions. *Methods Mol Biol* 1438:123–135. https://doi.org/10.1007/978-1-4939-3661-8_8.
- Grover M, Kashyap PC. 2014. Germ-free mice as a model to study effect of gut microbiota on host physiology. *Neurogastroenterol Motil* 26:745–748. <https://doi.org/10.1111/nmo.12366>.
- Sonnenburg JL, Chen CTL, Gordon JI. 2006. Genomic and metabolic studies of the impact of probiotics on a model gut symbiont and host. *PLoS Biol* 4:e413. <https://doi.org/10.1371/journal.pbio.0040413>.
- Alpert C, Scheel J, Engst W, Loh G, Blaut M. 2009. Adaptation of protein expression by *Escherichia coli* in the gastrointestinal tract of gnotobiotic mice. *Environ Microbiol* 11:751–761. <https://doi.org/10.1111/j.1462-2920.2008.01798.x>.
- Barroso-Batista J, Pedro MF, Sales-Dias J, Pinto CJG, Thompson JA, Pereira H, Demengeot J, Gordo I, Xavier KB. 2020. Specific eco-evolutionary contexts in the mouse gut reveal *Escherichia coli* metabolic versatility. *Curr Biol* 30:1049–1062.e7. <https://doi.org/10.1016/j.cub.2020.01.050>.
- Barroso-Batista J, Sousa A, Lourenço M, Bergman M-L, Sobral D, Demengeot J, Xavier KB, Gordo I. 2014. The first steps of adaptation of *Escherichia coli* to the gut are dominated by soft sweeps. *PLoS Genet* 10:e1004182. <https://doi.org/10.1371/journal.pgen.1004182>.
- Hill DR, Spence JR. 2017. Gastrointestinal organoids: understanding the molecular basis of the host-microbe interface. *Cell Mol Gastroenterol Hepatol* 3:138–149. <https://doi.org/10.1016/j.jcmgh.2016.11.007>.
- Min S, Kim S, Cho SW. 2020. Gastrointestinal tract modeling using organoids engineered with cellular and microbiota niches. *Exp Mol Med* 52:227–237. <https://doi.org/10.1038/s12276-020-0386-0>.
- Spence JR, Mayhew CN, Rankin SA, Kuhar M, Vallance JE, Tolle K, Hoskins EE, Kalinichenko VV, Wells SI, Zorn AM, Shroyer NF, Wells JM. 2011. Directed differentiation of human pluripotent stem cells into intestinal tissue in vitro. *Nature* 470:105–109. <https://doi.org/10.1038/nature09691>.
- Hill DR, Huang S, Nagy MS, Yadagiri VK, Fields C, Mukherjee D, Bons B, Dedhia PH, Chin AM, Tsai Y-H, Thodla S, Schmidt TM, Walk S, Young VB, Spence JR. 2017. Bacterial colonization stimulates a complex physiological response in the immature human intestinal epithelium. *Elife* 6:e29132. <https://doi.org/10.7554/eLife.29132>.
- McCracken KW, Howell JC, Wells JM, Spence JR. 2011. Generating human intestinal tissue from pluripotent stem cells in vitro. *Nat Protoc* 6:1920–1928. <https://doi.org/10.1038/nprot.2011.410>.
- Watson CL, Mahe MM, Múnera J, Howell JC, Sundaram N, Poling HM, Schweitzer JI, Vallance JE, Mayhew CN, Sun Y, Grabowski G, Finkbeiner SR, Spence JR, Shroyer NF, Wells JM, Helmrath MA. 2014. An in vivo model of human small intestine using pluripotent stem cells. *Nat Med* 20:1310–1314. <https://doi.org/10.1038/nm.3737>.
- Ochman H, Selander RK. 1984. Standard reference strains of *Escherichia coli* from natural populations. *J Bacteriol* 157:690–693. <https://doi.org/10.1128/JB.157.2.690-693.1984>.
- Gottesman S. 2019. Trouble is coming: signaling pathways that regulate general stress responses in bacteria. *J Biol Chem* 294:11685–11700. <https://doi.org/10.1074/jbc.REV119.005593>.
- Battesti A, Majdalani N, Gottesman S. 2011. The RpoS-mediated general stress response in *Escherichia coli*. *Annu Rev Microbiol* 65:189–213. <https://doi.org/10.1146/annurev-micro-090110-102946>.

20. Dong T, Joyce C, Schellhorn HE. 2008. The role of RpoS in bacterial adaptation, p 313–337. In El-Sharoud W (ed), *Bacterial physiology*. Springer, Berlin, Germany.
21. Dong T, Schellhorn HE. 2010. Role of RpoS in virulence of pathogens. *Infect Immun* 78:887–897. <https://doi.org/10.1128/IAI.00882-09>.
22. Price SB, Cheng C-M, Kaspar CW, Wright JC, DeGraves FJ, Penfound TA, Castanie-Cornet M-P, Foster JW. 2000. Role of rpoS in acid resistance and fecal shedding of *Escherichia coli* O157:H7. *Appl Environ Microbiol* 66:632–637. <https://doi.org/10.1128/AEM.66.2.632-637.2000>.
23. Krogfelt KA, Hjulgaard M, Sørensen K, Cohen PS, Givskov M. 2000. rpoS gene function is a disadvantage for *Escherichia coli* BJ4 during competitive colonization of the mouse large intestine. *Infect Immun* 68:2518–2524. <https://doi.org/10.1128/iai.68.5.2518-2524.2000>.
24. Trimble MJ, Mlynářčík P, Kolář M, Hancock REW. 2016. Polymyxin: alternative mechanisms of action and resistance. *Cold Spring Harb Perspect Med* 6:a025288. <https://doi.org/10.1101/cshperspect.a025288>.
25. Rahman M, Hasan MR, Oba T, Shimizu K. 2006. Effect of rpoS gene knockout on the metabolism of *Escherichia coli* during exponential growth phase and early stationary phase based on gene expressions, enzyme activities and intracellular metabolite concentrations. *Biotechnol Bioeng* 94:585–595. <https://doi.org/10.1002/bit.20858>.
26. Vijayakumar SR, Kirchhof MG, Patten CL, Schellhorn HE. 2004. RpoS-regulated genes of *Escherichia coli* identified by random lacZ fusion mutagenesis. *J Bacteriol* 186:8499–8507. <https://doi.org/10.1128/JB.186.24.8499-8507.2004>.
27. Pereira FC, Berry D. 2017. Microbial nutrient niches in the gut. *Environ Microbiol* 19:1366–1378. <https://doi.org/10.1111/1462-2920.13659>.
28. Sidar B, Jenkins BR, Huang S, Spence JR, Walk ST, Wilking JN. 2019. Long-term flow through human intestinal organoids with the gut organoid flow chip (GOFlowChip). *Lab Chip* 19:3552–3562. <https://doi.org/10.1039/c9lc00653b>.
29. Schwarz R, Kaspar A, Seelig J, Kunnecke B. 2002. Gastrointestinal transit times in mice and humans measured with ²⁷Al and ¹⁹F nuclear magnetic resonance. *Magn Reson Med* 48:255–261. <https://doi.org/10.1002/mrm.10207>.
30. Hugenholtz F, de Vos WM. 2018. Mouse models for human intestinal microbiota research: a critical evaluation. *Cell Mol Life Sci* 75:149–160. <https://doi.org/10.1007/s00018-017-2693-8>.
31. Conway T, Cohen PS. 2015. Commensal and pathogenic *Escherichia coli* metabolism in the gut. *Microbiol Spectr* 3:MBP-0006-2014. <https://doi.org/10.1128/microbiolspec.MBP-0006-2014>.
32. Crook N, Ferreiro A, Gasparrini AJ, Pesesky MW, Gibson MK, Wang B, Sun X, Conditte Z, Dobrowolski S, Peterson D, Dantas G. 2019. Adaptive strategies of the candidate probiotic *E. coli* Nissle in the mammalian gut. *Cell Host Microbe* 25:499–512.e8. <https://doi.org/10.1016/j.chom.2019.02.005>.
33. Okkelman IA, Neto N, Papkovsky DB, Monaghan MG, Dmitriev RI. 2020. A deeper understanding of intestinal organoid metabolism revealed by combining fluorescence lifetime imaging microscopy (FLIM) and extracellular flux analyses. *Redox Biol* 30:101420. <https://doi.org/10.1016/j.redox.2019.101420>.
34. Datsenko KA, Wanner BL. 2000. One-step inactivation of chromosomal genes in *Escherichia coli* K-12 using PCR products. *Proc Natl Acad Sci U S A* 97:6640–6645. <https://doi.org/10.1073/pnas.120163297>.
35. Dong T, Schellhorn HE. 2009. Global effect of RpoS on gene expression in pathogenic *Escherichia coli* O157:H7 strain EDL933. *BMC Genomics* 10:349. <https://doi.org/10.1186/1471-2164-10-349>.
36. Capeling M, Huang S, Mulero-Russe A, Cieza R, Tsai YH, Garcia A, Hill DR. 2020. Generation of small intestinal organoids for experimental intestinal physiology. *Methods Cell Biol* 159:143–174. <https://doi.org/10.1016/bs.mcb.2020.03.007>.
37. Ito A, May T, Taniuchi A, Kawata K, Okabe S. 2009. Localized expression profiles of rpoS in *Escherichia coli* biofilms. *Biotechnol Bioeng* 103:975–983. <https://doi.org/10.1002/bit.22305>.
38. Shiratsuchi A, Shimamoto N, Nitta M, Tuan TQ, Firdausi A, Gawasawa M, Yamamoto K, Ishihama A, Nakanishi Y. 2014. Role for σ^{38} in prolonged survival of *Escherichia coli* in *Drosophila melanogaster*. *J Immunol* 192:666–675. <https://doi.org/10.4049/jimmunol.1300968>.